

# Rotating Alfvén waves in rotating plasmas

J.-M. Rax <sup>1,2</sup>, R. Gueroult <sup>3,†</sup> and N.J. Fisch <sup>4</sup>

<sup>1</sup>Andlinger Center for Energy + the Environment, Princeton University, Princeton, NJ 08540, USA

<sup>2</sup>IJCLab, Université de Paris-Saclay, 91405 Orsay, France

<sup>3</sup>LAPLACE, Université de Toulouse, CNRS, INPT, UPS, 31062 Toulouse, France

<sup>4</sup>Department of Astrophysical Sciences, Princeton University, Princeton, NJ 08540, USA

(Received 19 September 2023; revised 28 November 2023; accepted 28 November 2023)

Angular momentum coupling between a rotating magnetized plasma and torsional Alfvén waves carrying orbital angular momentum (OAM) is examined. It is demonstrated not only that rotation is the source of Fresnel–Faraday rotation – or orbital Faraday rotation effects – for OAM-carrying Alfvén waves, but also that angular momentum from an OAM-carrying Alfvén wave can be transferred to a rotating plasma through the inverse process. For the direct process, the transverse structure angular rotation frequency is derived by considering the dispersion relation for modes with opposite OAM content. For the inverse process, the torque exerted on the plasma is derived as a function of wave and plasma parameters.

**Key words:** plasma waves, plasma dynamics

## 1. Introduction

Understanding the effect of rotation on plasma dynamics is essential to a wide range of applications. Besides original efforts motivated by microwave generation in magnetrons (Brillouin 1945), it has indeed been shown that rotation could enable new approaches to thermonuclear confinement (Wilcox 1959; Bekhtenev *et al.* 1980; Hassam 1997; Fetterman & Fisch 2008, 2010; Ochs & Fisch 2017; Rax, Gueroult & Fisch 2017). Rotation has also been found to hold promise for developing plasma mass separation applications (Gueroult *et al.* 2017, 2019*b*), either in pulsed plasma centrifuges (Bonnevier 1966; Krishnan, Geva & Hirshfield 1981) or in steady-state cross-field rotating plasmas (Ohkawa & Miller 2002; Shinohara & Horii 2007; Fetterman & Fisch 2011; Gueroult, Rax & Fisch 2014), advanced accelerators (Janes 1965; Janes, Levy & Petschek 1965; Janes *et al.* 1966; Rax & Robiche 2010; Thaury *et al.* 2013) and thrusters (Gueroult, Fruchtman & Fisch 2013). But understanding the effect of rotation on plasma dynamics is also essential in a number of environments. Rotation is for instance key to the structure and stability of a number of astrophysical objects (Kulsrud 1999; Miesch & Toomre 2009). In light of this ubiquitousness, and because plasma waves are widely used for both control and diagnostics in plasmas, it seems desirable to understand what the effect of rotation on wave

† Email address for correspondence: [renaud.gueroult@laplace.univ-tlse.fr](mailto:renaud.gueroult@laplace.univ-tlse.fr)

propagation in plasmas may be (Gueroult, Rax & Fisch 2023). In fact the importance of this task was long recognized in geophysics and astrophysics, leading to extensive studies of low-frequency magnetohydrodynamic (MHD) waves in rotating plasmas (Lehnert 1954; Hide 1969; Acheson 1972; Acheson & Hide 1973; Campos 2010), and notably of Alfvén waves (Stix 1992).

Meanwhile, following the discovery that electromagnetic waves carry both spin and orbital angular momentum (Allen *et al.* 1992; Andrews & Babiker 2012; Allen, Barnett & Padgett 2016), there have been numerous theoretical developments on spin-orbit interactions (Bliokh *et al.* 2015) in modern optics, which we note are now being applied to plasmas (Bliokh & Bliokh 2022). For spin angular momentum (SAM)-carrying waves, that is, circularly polarized waves, propagation through a rotating medium is known to lead to a phase shift between eigenmodes with opposite SAM content (Player 1976; Gueroult *et al.* 2019a; Gueroult, Rax & Fisch 2020). This phase shift is then the source of a rotation of polarization or polarization drag (Jones 1976), as originally postulated by Thomson (1885) and Fermi (1923). For orbital angular momentum (OAM)-carrying waves, propagation through a rotating medium is the source of a phase shift between eigenmodes with opposite OAM content (Götte, Barnett & Padgett 2007), leading to image rotation or Faraday–Fresnel rotation (Padgett *et al.* 2006).

This azimuthal Fresnel drag of OAM-carrying waves, which can be viewed as an orbital Faraday rotation of the amplitude, was first derived (Wisniewski-Barker *et al.* 2014) and observed (Franke-Arnold *et al.* 2011) in isotropic, non-gyrotropic media. In contrast, propagation of OAM-carrying waves in a rotating anisotropic (gyrotropic) medium poses greater difficulty since the polarization state and the wave vector direction – which are independent parameters for a given wave frequency in an isotropic medium – become coupled. Yet, it was recently shown that Faraday–Fresnel rotation is also found for the high-frequency magnetized plasma modes that are Whistler–Helicon and Trivelpiece–Gould modes (Rax & Gueroult 2021). For such high-frequency modes it was found that the main modifications induced by the plasma rotation are associated with Doppler shift and Coriolis effect in the dispersion relation. Interestingly, we note that the result that rotation is the source of an azimuthal component for the group velocity of low-frequency waves in magnetized plasmas when  $\boldsymbol{\Omega} \cdot \mathbf{k} \neq 0$  was already pointed out in geophysics and astrophysics (Acheson & Hide 1973), but the connection to a Faraday–Fresnel rotation of the transverse structure of the wave did not seem to have been made. An added complexity for these low-frequency modes is that one must, in addition to anisotropy and gyrotropy, consider the strong coupling to the inertial mode (Lighthill 1980) that then comes into play. Revisiting this problem, we derive here in this study the expression for Faraday–Fresnel rotation for low-frequency rotating Alfvén waves in a rotating magnetized plasma.

This paper is organized as follows. After briefly recalling the configuration of interest and previous results in the next section, we construct in § 3 the spectrum of low-frequency, small-amplitude, fluid waves in a magnetized rotating plasma. The set of linearized Euler and Maxwell equations describes an oscillating Beltrami flow-force-free field (Chandrasekhar & Prendergast 1956) whose components are expressed with a cylindrical Chandrasekhar–Kendall (CK) potential (Chandrasekhar & Kendall 1957; Yoshida 1991). Then, in § 4, these OAM-carrying waves are shown to display a Faraday–Fresnel rotation under the influence of the plasma rotation. Section 5 focuses on the inverse problem when the OAM of the wave is absorbed by the plasma. We derive in this case the torque exerted by this wave on the fluid driven as a function of the wave and plasma parameters. Finally § 6 summarizes the main findings of this study.

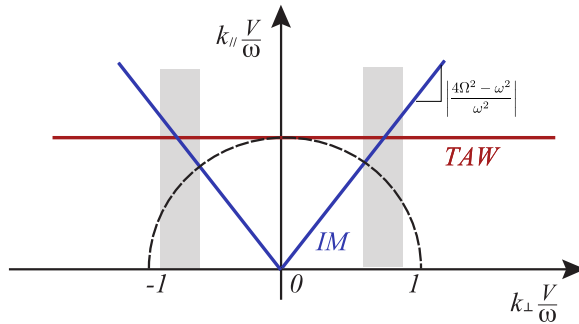


FIGURE 1. Uncoupled dispersion of torsional Alfvén waves (TAW) obtained for  $B_0 \neq 0$  and  $\Omega = 0$  and of inertial waves (IM) obtained for  $\Omega \neq 0$  and  $B_0 = 0$ .

### 2. Background

In this study we consider a rotating magnetized plasma column with constant angular velocity  $\Omega = \Omega e_z$  and static uniform magnetic field  $B_0 = B_0 e_z$ . We write  $(r, \theta, z)$  cylindrical coordinates on a cylindrical basis  $(e_r, e_\theta, e_z)$ . The plasma dynamics is described assuming an inviscid and incompressible fluid model. We classically define the Alfvén velocity

$$V \doteq B_0 / \sqrt{\mu_0 \rho}, \tag{2.1}$$

where  $\mu_0$  is the permittivity of vacuum and  $\rho$  the mass density of the fluid.

In the simple case where  $B_0 = 0$  and  $\Omega \neq 0$  the rotating plasma behaves as an ordinary rotating fluid and inertial waves can propagate. Taking a phase factor  $\exp j(\omega t - k_{\parallel} z - k_{\perp} y)$ , the dispersion relation for this inertial mode is (Lighthill 1980)

$$\omega = \pm 2\Omega k_{\parallel} / \sqrt{k_{\parallel}^2 + k_{\perp}^2}. \tag{2.2}$$

Conversely, in the case where  $\Omega = 0$  but  $B_0 \neq 0$ , Alfvén waves can propagate in the magnetized plasma at rest. The dispersion of this torsional mode is (Stix 1992)

$$\omega = \pm B_0 k_{\parallel} / \sqrt{\mu_0 \rho} = \pm k_{\parallel} V. \tag{2.3}$$

Note that compressional Alfvén waves are not considered here as we are considering an incompressible plasma. The dispersion of uncoupled torsional Alfvén waves and inertial waves is plotted in figure 1 in the  $(k_{\parallel} V / \omega, k_{\perp} V / \omega)$  plane for a given frequency  $\omega$ . Note that we have normalized for convenience the wavevector to  $\omega / V$ , and that even for the unmagnetized inertial wave branch.

In the more general case where both  $B_0 \neq 0$  and  $\Omega \neq 0$ , then a strong coupling between inertial waves and torsional Alfvén waves modes rearranges the spectrum and gives rise to two new branches (Lehnert 1954; Acheson & Hide 1973). This coupling is expected to be strongest in the regions where the the dispersion curves of the modes absent rotation (torsional Alfvén waves) and absent magnetic field (inertial waves) intersect, which is highlighted in grey in figure 1. Since as already pointed out by Acheson & Hide (1973) the group velocity of these new modes for waves such that  $\Omega \cdot k \neq 0$  has an azimuthal component, then we expect Fresnel–Faraday rotation as recently identified for Trivelpiece–Gould and Whistler–Helicon high-frequency electronic modes (Rax & Gueroult 2021).

### 3. Rotating Alfvén waves in a rotating plasma

In this section we examine the properties of low-frequency waves carrying OAM in a rotating magnetized plasma.

#### 3.1. Classical modes

Two methods can be used to identify and describe the coupling between the angular momentum of a rotating plasma column and the angular momentum of a wave propagating in this rotating magnetized plasma. One is to consider the transformation laws of the various parameters from the laboratory frame to a rotating frame. The other is to perform the study in the laboratory frame starting from first principles. Here we use the first method, similarly to original contributions on MHD waves in rotating conductive fluids (Lehnert 1954; Hide 1969), and solve the perfect MHD dynamics to calculate the rotating plasma linear response for the low-frequency branches where the coupling between the fields and the particles is large. By working in the co-rotating frame ( $R$ ) rather than in the laboratory frame ( $L$ ), both the Coriolis force  $2\boldsymbol{\Omega} \times \mathbf{v}$  and the centrifugal forces  $-\nabla\psi$  with  $\psi = -\Omega^2 r^2/2$  must be taken into account.

We model the evolution of the wave velocity field  $\mathbf{v}(\mathbf{r}, t)$  using Euler's equation under the assumptions of homogeneity and zero viscosity:

$$\frac{\partial \mathbf{v}}{\partial t} + (\mathbf{v} \cdot \nabla) \mathbf{v} + 2\boldsymbol{\Omega} \times \mathbf{v} = -\nabla \left( \frac{P}{\rho} + \psi \right) + \frac{1}{\mu_0 \rho} (\nabla \times \mathbf{B}) \times (\mathbf{B} + \mathbf{B}_0) \quad (3.1)$$

and the evolution of the wave magnetic field  $\mathbf{B}(\mathbf{r}, t)$  using the Maxwell–Faraday equation under the assumption of perfect conductivity:

$$\frac{\partial \mathbf{B}}{\partial t} = \nabla \times [\mathbf{v} \times (\mathbf{B} + \mathbf{B}_0)], \quad (3.2)$$

where  $\rho$  is the mass density of the fluid and  $P$  is the pressure. These dynamical relations are completed by the flux conservation law

$$\nabla \cdot \mathbf{B} = 0 \quad (3.3)$$

for the magnetic field and the incompressibility relation

$$\nabla \cdot \mathbf{v} = 0 \quad (3.4)$$

for the velocity field. As already mentioned, this last relation will restrict the plasma behaviour to the Alfvénic dynamics associated with torsional waves. We should also stress that the assumptions made here and in this study only capture specific kinds of pressure equilibrium. Indeed a rotating equilibrium demands a radial gradient in the total pressure (that is either in the plasma pressure or in the magnetic pressure) to balance the centrifugal forces (Hameiri 1983). In bringing the density under the gradient in (3.1), which will facilitate the analysis of perturbations around this equilibrium, we implicitly assumed a homogeneous density. In this model the pressure gradient must thus come entirely from a temperature gradient. Although restrictive, we work here within this homogeneous assumption to expose new coupling phenomena, and keep in mind that this is only an approximation whose justification remains to be demonstrated.

We now consider a small-amplitude MHD perturbation, propagating along and around the  $z$  axis, described by a magnetic perturbation:

$$\mathbf{B}(r, \theta, z, t) = \mathfrak{B}(r, \theta, z) \exp(j\omega t) \quad (3.5)$$

with respect to the uniform static magnetic field  $\mathbf{B}_0 = B_0 \mathbf{e}_z$ . The wave frequency  $\omega$  is assumed smaller than the ion cyclotron frequency and larger than the collision frequency to validate the use of the perfect MHD model (3.1), (3.2). The oscillating magnetic wave  $\mathbf{B}$  is associated with an oscillating hydrodynamic velocity perturbation  $\mathbf{v}$ :

$$\mathbf{v}(r, \theta, z, t) = \mathbf{u}(r, \theta, z) \exp(j\omega t) \quad (3.6)$$

with respect to rotating frame velocity equilibrium  $\mathbf{v}_0 = \mathbf{0}$ . The pressure  $P$  balances the centrifugal force at equilibrium  $\nabla(P + \rho\psi) = \mathbf{0}$  and the pressure perturbation is  $p(r, \theta, z) \exp j\omega t$ . To first order in these perturbations, the linearization of (3.1) and (3.2) gives

$$j\omega \mathbf{u} + 2\boldsymbol{\Omega} \times \mathbf{u} = -\nabla(p/\rho) + \frac{1}{\mu_0 \rho} (\nabla \times \mathfrak{B}) \times \mathbf{B}_0, \quad (3.7)$$

$$j\omega \mathfrak{B} = (\mathbf{B}_0 \cdot \nabla) \mathbf{u}. \quad (3.8)$$

Flux conservation and incompressibility provide the two additional conditions

$$\nabla \cdot \mathbf{u} = 0, \quad (3.9)$$

$$\nabla \cdot \mathfrak{B} = 0. \quad (3.10)$$

Taking the curl of both (3.7) and (3.8) and eliminating  $\mathfrak{B}$  gives a linear relation for the velocity perturbation:

$$\omega^2 \nabla \times \mathbf{u} + 2j\omega (\boldsymbol{\Omega} \cdot \nabla) \mathbf{u} + (V \cdot \nabla)^2 (\nabla \times \mathbf{u}) = \mathbf{0}, \quad (3.11)$$

with  $V$  the Alfvén velocity already defined in (2.1). Note that the elimination of the pressure term obtained by taking the curl of (3.7) would not be possible if, as hinted at earlier, accounting for a radial density gradient.

Now if one Fourier-analyses this velocity perturbation as a superposition of plane waves:

$$\mathbf{u}(\mathbf{r}) \exp j\omega t = \exp[j(\omega t - \mathbf{k} \cdot \mathbf{r})], \quad (3.12)$$

that is to say put the emphasis on the linear momentum dynamics rather than on the angular momentum dynamics, one recovers the two branches of Alfvénic/inertial perturbations in a rotating plasma (Lehnert 1954; Acheson & Hide 1973). Specifically, plugging (3.12) into (3.11) and then taking the cross-product  $j\mathbf{k} \times$  of this algebraic relation, one obtains the dispersion relation

$$\omega^2 - (\mathbf{k} \cdot \mathbf{V})^2 = \pm 2\omega (\boldsymbol{\Omega} \cdot \mathbf{k}) / |\mathbf{k}|. \quad (3.13)$$

The two solutions, which are illustrated in figure 2, have been widely investigated within the context of geophysical and astrophysical MHD models. They are also in agreement with the solutions obtained from the local dispersion relation for magneto-rotational instabilities (Goedbloed, Keppens & Poedts 2019, § 13.5.1) in the appropriate limit. For short wavelengths, the  $\Omega = 0$  torsional Alfvén wave splits into an inertial and a magneto-inertial wave. For long wavelengths, that is, in the grey zone in figure 2, inertial terms dominate the dispersion and the inertial wave is found to reduce to its zero

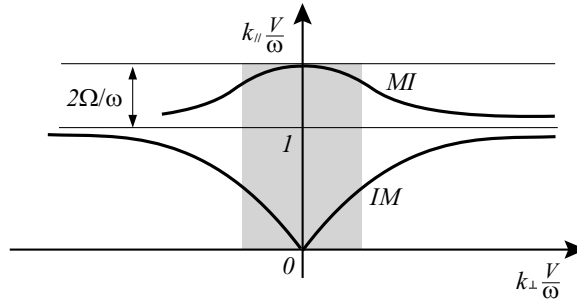


FIGURE 2. Coupled dispersion of magneto-inertial waves (MI) and inertial waves (IM).

rotation behaviour already shown in [figure 1](#). Note finally that the torsional Alfvén wave is recovered for large  $k_{\perp}$  where a local dispersion becomes valid as opposed to small  $k_{\perp}$  where the large wavelength allows the wave to probe the large-scale behaviour of the rotation.

### 3.2. Beltrami flow

Instead of this usual procedure using a full Fourier decomposition as given by (3.12), we start here by considering a travelling perturbation along  $z$  of the form

$$\mathbf{u}(r, \theta, z) = \mathbf{w}(r, \theta) \exp(-jk_{\parallel}z). \quad (3.14)$$

Note that this is analogous to what was already done by Shukla (2012) to study OAM-carrying dispersive shear Alfvén waves, though in this earlier study the paraxial approximation and a two-fluid model were used, and the plasma was considered at rest (i.e. non-rotating). Plugging (3.14) in the dispersion relation for a rotating plasma (3.11) gives

$$\nabla \times \mathbf{u} = \mathcal{K}\mathbf{u}, \quad (3.15)$$

where we have defined

$$\mathcal{K}(k_{\parallel}, \omega) \doteq 2\frac{\Omega}{\omega}k_{\parallel} \left( \frac{k_{\parallel}^2 V^2}{\omega^2} - 1 \right)^{-1}. \quad (3.16)$$

From (3.8) the oscillating magnetic field is then written as

$$\omega \mathfrak{B} = -\sqrt{\mu_0 \rho} k_{\parallel} V \mathbf{u}. \quad (3.17)$$

The two modes identified in [figure 2](#) can be recovered from (3.16). More specifically, for  $k_{\parallel}V > \omega$  (3.15) describes an Alfvén wave modified by inertial effect. Conversely for  $k_{\parallel}V < \omega$  (3.15) describes an inertial wave modified by MHD coupling. In the following we focus on the Alfvén wave dynamics and thus assume  $\mathcal{K} > 0$ .

Equation (3.15) is characteristic of a Beltrami flow (Chandrasekhar & Prendergast 1956). As such  $\mathbf{u}$  can be written in terms of the so-called CK potential  $\Phi$  (Chandrasekhar

& Kendall 1957) as

$$\begin{aligned} \mathbf{u} &= \frac{1}{\mathcal{K}} \nabla \times (\nabla \times \Phi \mathbf{e}_z) + \nabla \times \Phi \mathbf{e}_z \\ &= - \left[ \frac{1}{\mathcal{K}} \nabla \times \mathbf{e}_z \times \nabla + \mathbf{e}_z \times \nabla \right] \Phi, \end{aligned} \tag{3.18}$$

where the CK potential is a solution of the scalar Helmholtz equation

$$\Delta \Phi + \mathcal{K}^2 \Phi = 0. \tag{3.19}$$

One verifies that the three components of (3.18) are independent.

Before examining the structure of OAM-carrying modes through the CK potential, two additional results can be obtained from (3.16). First, for the Fourier decomposition used above, plugging (3.13) in (3.16) gives

$$\frac{\mathcal{K}^2}{k_{\parallel}^2} = 1 + \frac{k_{\perp}^2}{k_{\parallel}^2} > 1. \tag{3.20}$$

Second, we can derive the dimensionless group-velocity dispersion coefficient

$$\frac{\omega}{\mathcal{K}} \frac{\partial \mathcal{K}}{\partial \omega} = - \frac{k_{\parallel}}{\mathcal{K}} \frac{\partial \mathcal{K}}{\partial k_{\parallel}} = \frac{k_{\parallel}^2 V^2 + \omega^2}{k_{\parallel}^2 V^2 - \omega^2}, \tag{3.21}$$

which we use later to make explicit the axial wavevector difference for two eigenmodes with opposite OAM content.

### 3.3. Structure of OAM-carrying modes

Because we are interested in waves carrying OAM around  $z$  and linear momentum along  $z$ , we search for solutions of the form

$$\Phi(r, \theta, z) = \phi(r) \exp[-j(m\theta + k_{\parallel}z)], \tag{3.22}$$

where  $m \in \mathbb{Z}$  is the azimuthal mode number associated with the OAM of the wave. From (3.19) the radial amplitude of this rotating CK potential  $\phi(r)$  must be a solution of the Bessel equation

$$\frac{1}{r} \frac{d}{dr} \left( r \frac{d\phi}{dr} \right) - \frac{m^2}{r^2} \phi + (\mathcal{K}^2 - k_{\parallel}^2) \phi = 0. \tag{3.23}$$

Since as shown in (3.20)  $\mathcal{K}^2 > k_{\parallel}^2$ ,  $\phi(r)$  is in general the combination of Bessel functions of the first and the second kind and order  $m \in \mathbb{Z}$ ,  $J_m$  and  $Y_m$ . Yet, the finite value of  $\phi$  at  $r = 0$  demands restricting the physical solution to Bessel functions of the first kind  $J_m$  so that we find

$$\phi(r) = J_m(\alpha r), \tag{3.24}$$

with the cylindrical dispersion relation

$$\alpha^2 + k_{\parallel}^2 = \mathcal{K}^2(k_{\parallel}, \omega). \tag{3.25}$$

Note that, like the ordinary plane wave (3.12) used in the standard analysis, the cylindrical Bessel waves (3.24) cannot be normalized.

Putting these pieces together one finally gets

$$\begin{aligned} \mathbf{v} &= \left[ \frac{1}{\mathcal{K}} \nabla \times \mathbf{e}_z \times \nabla + \mathbf{e}_z \times \nabla \right] J_m(\sqrt{\mathcal{K}^2 - k_{\parallel}^2} r) \exp[j(\omega t - m\theta - k_{\parallel} z)] \\ &= -\frac{\omega \mathbf{B}}{\sqrt{\mu_0 \rho} k_{\parallel} V}. \end{aligned} \tag{3.26}$$

The components in the plasma frame of a rotating Alfvén wave with azimuthal mode number  $m$  thus have an amplitude proportional to combination of Bessel functions of the first kind and of orders  $m$  and  $m \pm 1$ . All these Bessel functions have the same radial dependence, namely  $\sqrt{\mathcal{K}^2(k_{\parallel}, \omega) - k_{\parallel}^2} r$ , where  $\mathcal{K}(k_{\parallel}, \omega)$  is given by (3.16).

#### 4. Direct rotational Fresnel drag–orbital Faraday rotation

Let us now rewrite these perturbations as seen from the laboratory frame. We use the index  $R$  for the rotating plasma rest frame and  $L$  for the laboratory frame. The radial Eulerian coordinates  $r$  and  $z$  are unchanged through this change of frame or reference, but the azimuthal coordinate  $\theta$  changes, with

$$r|_L = r|_R, \tag{4.1}$$

$$z|_L = z|_R, \tag{4.2}$$

$$\theta|_L = \theta|_R + \Omega t. \tag{4.3}$$

Since the axial wavevector is unchanged  $k_{\parallel}|_R = k_{\parallel}|_L$ , the phase of the wave in the plasma rest frame

$$\omega t - k_{\parallel} z \pm m\theta|_R \tag{4.4}$$

becomes

$$(\omega \mp m\Omega)t - k_{\parallel} z \pm m\theta|_L \tag{4.5}$$

in the laboratory frame.

Equipped with these transformations we can now describe the conditions to observe Fresnel–Faraday rotation. For this we consider two CK potentials describing two Alfvén modes with opposite OAM content in the rotating frame  $R$ :

$$\left. \begin{aligned} \Phi_{+}|_R &= J_m(\alpha r) \exp(j[(\omega - m\Omega)t - (k_{\parallel} - \delta k_{\parallel})z - m\theta|_R]), \\ \Phi_{-}|_R &= J_{-m}(\alpha r) \exp(j[(\omega + m\Omega)t - (k_{\parallel} + \delta k_{\parallel})z + m\theta|_R]). \end{aligned} \right\} \tag{4.6}$$

These transform in the CK potentials in the laboratory frame  $L$ :

$$\left. \begin{aligned} \Phi_{+}|_L &= J_m(\alpha r) \exp(j[\omega t - (k_{\parallel} - \delta k_{\parallel})z - m\theta|_L]), \\ \Phi_{-}|_L &= J_{-m}(\alpha r) \exp(j[\omega t - (k_{\parallel} + \delta k_{\parallel})z + m\theta|_L]), \end{aligned} \right\} \tag{4.7}$$

as a result of the rotational Doppler shift  $\theta|_L = \theta|_R + \Omega t$ . These Alfvén CK potentials  $\Phi_{\pm}|_L$  can be driven by a multicoil antenna similar to that used to study Whistler–Helicon modes (Stenzel & Urrutia 2014, 2015a,b,c; Urrutia & Stenzel 2015, 2016; Stenzel & Urrutia 2018; Stenzel 2019). The radial field pattern is then a superposition of  $+m$  and  $-m$  Bessel amplitudes  $J_{\pm m}(\alpha r)$ , where  $\alpha$  is associated with the radial modulation of the antenna currents (Rax & Gueroult 2021). The antenna then sets both the radial wavevector

$\alpha$  and the frequency  $\omega$ , whereas the axial wavevectors  $k_{\parallel} \pm \delta k_{\parallel}$  are solutions of the rotating frame dispersion relation. From (3.25),

$$\alpha = \sqrt{\mathcal{K}^2(k_{\parallel} - \delta k_{\parallel}, \omega - m\Omega) - (k_{\parallel} - \delta k_{\parallel})^2}, \tag{4.8}$$

$$\alpha = \sqrt{\mathcal{K}^2(k_{\parallel} + \delta k_{\parallel}, \omega + m\Omega) - (k_{\parallel} + \delta k_{\parallel})^2}. \tag{4.9}$$

Since we assume  $\omega \gg \Omega$  and  $k_{\parallel} \gg \delta k_{\parallel}$ , we can Taylor-expand (4.8) and (4.9) to get  $\delta k_{\parallel}$ , leading to

$$\frac{k_{\parallel}}{\mathcal{K}} \delta k_{\parallel} = \frac{\delta k_{\parallel}}{2} \frac{\partial \mathcal{K}(\omega, k_{\parallel})}{\partial k_{\parallel}} + \frac{m\Omega}{2} \frac{\partial \mathcal{K}(\omega, k_{\parallel})}{\partial \omega}. \tag{4.10}$$

Equation (3.21) can then be used to finally write the axial wavevector difference  $\delta k_{\parallel}$  for two modes with the same frequency  $\omega$ , the same radial amplitude  $|J_m(\alpha r)|$  and equal but opposite azimuthal number  $|m|$  as

$$\frac{\delta k_{\parallel}}{k_{\parallel}} = \frac{1}{2} m \frac{\Omega}{\omega} \frac{1 + \frac{k_{\parallel}^2 V^2}{\omega^2}}{1 - \frac{k_{\parallel}^2}{\mathcal{K}^2} + \left(1 + \frac{k_{\parallel}^2}{\mathcal{K}^2}\right) \frac{k_{\parallel}^2 V^2}{\omega^2}}, \tag{4.11}$$

where  $\mathcal{K}(k_{\parallel}, \omega, \Omega)$  is given by (3.16). This implies that there will be a difference in the axial phase velocity  $\omega/(k_{\parallel} \pm \delta k_{\parallel})$  of these two modes, and because these two modes rotate in opposite directions due to their opposite azimuthal mode number, the transverse structure of the sum of these modes will rotate. This is the Fresnel drag–Faraday orbital rotation effect. Specifically, if one launches a wave which is a superposition of  $+m$  and  $-m$  modes such that at the antenna location  $z = 0$

$$\Phi|_{z=0} = J_m(\alpha r) ((\exp[j(\omega t - m\theta|_L)]) + (-1)^m \exp[j(\omega t + m\theta|_L)]), \tag{4.12}$$

the wave transverse amplitude rotates as it propagates along  $z > 0$  with an angular velocity along the propagation axis

$$\frac{d\theta}{dz}|_L = \frac{\delta k}{m} = \frac{1}{2} \frac{\Omega}{\omega} k_{\parallel} \mathcal{K}^2 \frac{k_{\parallel}^2 V^2 + \omega^2}{k_{\parallel}^2 V^2 (\mathcal{K}^2 + k_{\parallel}^2) + \omega^2 (\mathcal{K}^2 - k_{\parallel}^2)}. \tag{4.13}$$

This CK potential rotation is illustrated in figure 3 for the case  $m = 4$ . Equations (4.11) and (4.13) quantify the direct Faraday–Fresnel effect of Alfvén waves in rotating plasmas, completing the similar results previously obtained for Trivelpiece–Gould and Whistler–Helicon modes (Rax & Gueroult 2021). The  $1/m$  factor in (4.13) comes from the fact that the image constructed from the superposition of  $\pm m$  modes has a  $2m$ -fold symmetry.

To conclude this section it was shown that besides the Fresnel–Faraday rotation associated with a phase-velocity difference for  $m$  and  $-m$  modes, there can also be a splitting of the envelope of an  $(m, -m)$  wave packet if the group velocity for co-rotating ( $m$ ) and counter-rotating ( $-m$ ) modes were different (Rax & Gueroult 2021). We note that this second effect is also present here for Alfvén waves in rotating plasmas. Indeed, given

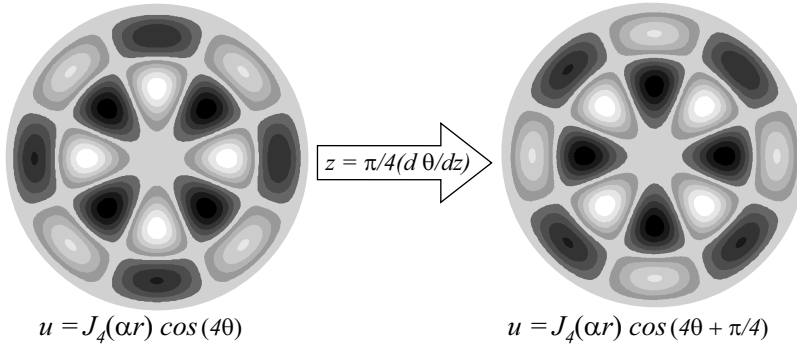


FIGURE 3. Fresnel drag–Faraday rotation of the CK potential describing an Alfvén–Beltrami wave with  $m = \pm 4$  after a propagation along a path  $z = \pi/4(d\theta/dz)$ .

a radial wavevector  $\alpha$  the dispersion relation is  $\mathcal{D} = \mathcal{K}^2 - k_{\parallel}^2 - \alpha^2 = 0$ , so that from (3.21) the axial group velocity is given by

$$-\frac{\partial \mathcal{D}}{\partial k_{\parallel}} / \frac{\partial \mathcal{D}}{\partial \omega} = \frac{k_{\parallel}}{\mathcal{K} \partial \mathcal{K} / \partial \omega} - \frac{\omega}{k_{\parallel}}, \tag{4.14}$$

and one verifies from (3.16) that the group velocity for a mode  $(k_{\parallel} + \delta k_{\parallel}, m)$  and that for a mode  $(k_{\parallel} - \delta k_{\parallel}, -m)$  are different. Rather than deriving here an explicit formula for the Fresnel–Faraday splitting, we consider in the next section the inverse Fresnel–Faraday effect associated with wave absorption.

### 5. Inverse rotational Fresnel drag and angular momentum absorption

In a perfectly conducting inviscid plasma there is no power absorption. The power exchange between the oscillating electromagnetic field and the plasma is purely reactive. To obtain an irreversible (active) angular momentum absorption, one needs a dissipative mechanism. Two different wave OAM absorption mechanisms can be considered. One is resonant collisionless absorption; the other is collisional absorption. The former was recently studied in Rax, Gueroult & Fisch (2023) through quasilinear theory and will not be considered here. Instead, we consider in this section a weakly dissipative plasma where the ideal MHD hypothesis of perfect conductivity is relaxed and the inviscid assumption of zero viscosity no longer applies. In both cases, collisional or collisionless, each time an energy  $\delta \mathcal{U}$  is absorbed by the plasma, an axial angular momentum  $\delta L = m \delta \mathcal{U} / \omega$  is also absorbed by the plasma (Rax *et al.* 2017, 2023). The rate of decay of the wave angular momentum is hence equal to the wave-induced density of torque on the plasma  $\Gamma = dL/dt$ . In steady state, this angular momentum transfer  $d\Gamma/dt$  is balanced by viscous damping of the velocity shear and Ohmic dissipation of the radial charge polarization sustaining the rotation. This dissipation is larger in the collisional case considered here than in the collisionless regime considered in Rax *et al.* (2023).

Specifically, we introduce two dissipative collisional couplings to our dissipation-less system (3.7), (3.8), namely finite viscosity  $\rho \mu$  and finite resistivity  $\mu_0 \eta$ . We follow the notation of Taylor (1989) (devoted to Alfvén wave helicity absorption) and introduce the magnetic diffusion coefficient  $\eta$  and the kinematic viscosity  $\mu$ . Ohm’s law is then written

as  $\mathbf{E} + \mathbf{v} \times \mathbf{B} = \mu_0 \eta \mathbf{j}$  and the system (3.7), (3.8) becomes

$$j\omega \mathbf{u} + 2\boldsymbol{\Omega} \times \mathbf{u} = -\nabla(p/\rho) + \frac{1}{\mu_0 \rho} (\nabla \times \mathfrak{B}) \times \mathbf{B}_0 + \mu \Delta \mathbf{u}, \tag{5.1}$$

$$j\omega \mathfrak{B} = (\mathbf{B}_0 \cdot \nabla) \mathbf{u} + \eta \Delta \mathfrak{B}. \tag{5.2}$$

Since we assume weak dissipation, the resistive term  $\eta \Delta \mathbf{B}$  in the Maxwell–Faraday equation and the viscous term  $\mu \Delta \mathbf{u}$  in the Navier–Stokes equation can be evaluated with the dispersive properties of the non-dissipative dispersion relation. Within the bounds of this perturbative expansion scheme ( $\mathcal{K}^2 \eta \ll \omega$  and  $\mathcal{K}^2 \mu \ll \omega$ ), and for the perturbation  $\mathbf{u}(r, \theta, z) = \mathbf{w}(r, \theta) \exp(-jk_{\parallel} z)$  already given in (3.14), we get from (3.15), (3.17) the non-dissipative Laplacians

$$\Delta \mathbf{u} = -\mathcal{K}^2 \mathbf{u}, \tag{5.3}$$

$$\Delta \mathfrak{B} = -\mathcal{K}^2 \mathfrak{B}. \tag{5.4}$$

Plugging these results into (5.1), (5.2) yields the system

$$j\omega \mathbf{u} + 2\boldsymbol{\Omega} \times \mathbf{u} = -\nabla(p/\rho) + \frac{1}{\mu_0 \rho} (\nabla \times \mathfrak{B}) \times \mathbf{B}_0 - \mathcal{K}^2 \mu \mathbf{u}, \tag{5.5}$$

$$j\omega \mathfrak{B} = (\mathbf{B}_0 \cdot \nabla) \mathbf{u} - \mathcal{K}^2 \eta \mathfrak{B}, \tag{5.6}$$

where now viscous and resistive dissipation introduce a local relaxation.

We then take the rotational of the first equation and eliminate  $\mathfrak{B}$  using the second equation to get

$$[(j\omega + \mathcal{K}^2 \mu)(j\omega + \mathcal{K}^2 \eta)] \nabla \times \mathbf{u} + 2j(j\omega + \mathcal{K}^2 \eta) k_{\parallel} \Omega \mathbf{u} + k_{\parallel}^2 V^2 \nabla \times \mathbf{u} = \mathbf{0}. \tag{5.7}$$

After some algebra we find that the linearized dissipative regime of velocity and field low-frequency oscillations is now described by

$$\nabla \times \mathbf{u} = [\mathcal{K}_R(k_{\parallel}, \omega) - j\mathcal{K}_I(k_{\parallel}, \omega)] \mathbf{u}, \tag{5.8}$$

$$(\omega - j\mathcal{K}^2 \eta) \mathbf{B} = -\sqrt{\mu_0 \rho} k_{\parallel} V \mathbf{u}, \tag{5.9}$$

rather than by the collisionless equations (3.15), (3.17), where we have defined the two real wavevectors  $\mathcal{K}_R \approx \mathcal{K} \gg \mathcal{K}_I$  through

$$\mathcal{K}_R(k_{\parallel}, \omega) - j\mathcal{K}_I(k_{\parallel}, \omega) = 2\Omega \frac{(\omega - j\mathcal{K}^2 \eta) k_{\parallel}}{k_{\parallel}^2 V^2 - (\omega - j\mathcal{K}^2 \mu)(\omega - j\mathcal{K}^2 \eta)}. \tag{5.10}$$

We then consider an initial-value problem with a weakly decaying wave of the form

$$\mathbf{v} = \mathbf{u} \exp[j(\omega + j\nu)t], \tag{5.11}$$

with  $\omega \gg \nu$ , and with the structure

$$\mathbf{v} = \left[ \frac{1}{\mathcal{K}_R - j\mathcal{K}_I} \nabla \times \mathbf{e}_z \times \nabla + \mathbf{e}_z \times \nabla \right] J_m(\alpha r) \exp(j[(\omega + j\nu)t - m\theta - k_{\parallel} z]), \tag{5.12}$$

where  $\alpha$  is a real number,  $\omega$  and  $k_{\parallel}$  are given and the damping rate  $\nu(\omega, k_{\parallel}, \mathcal{K})$  is to be determined from the weak dissipation expansion of the dispersion relation

$$\alpha^2 + k_{\parallel}^2 = [\mathcal{K}_R(k_{\parallel}, \omega + j\nu) - j\mathcal{K}_I(k_{\parallel}, \omega + j\nu)]^2, \tag{5.13}$$

obtained by plugging this solution in (5.8). Taylor-expanding this last relation for  $v \ll \omega$ , the lowest-order real part gives the collisionless dispersion

$$\alpha^2(k_{\parallel}, \omega) = \mathcal{K}_R^2(k_{\parallel}, \omega) - k_{\parallel}^2 \approx \mathcal{K}^2(k_{\parallel}, \omega) - k_{\parallel}^2, \tag{5.14}$$

while the lowest-order imaginary part gives a relation for the decay rate  $\nu$ :

$$\nu(k_{\parallel}, \omega) \frac{\partial \mathcal{K}_R(\omega)}{\partial \omega} = \mathcal{K}_I(k_{\parallel}, \omega) \approx \frac{\mathcal{K}^3}{\omega} \left[ \eta + (\mu + \eta) \left( \frac{k_{\parallel}^2 V^2}{\omega^2} - 1 \right)^{-1} \right]. \tag{5.15}$$

Here we took  $\partial \mathcal{K}_R / \partial \omega \approx \partial \mathcal{K} / \partial \omega$  and used (3.21).

Finally, (5.15) can be used to write an equation for the evolution of the wave energy density  $\mathcal{U}$ :

$$\frac{d\mathcal{U}}{dt} = -2\nu\mathcal{U} = -2\mathcal{K}_I \left( \frac{\partial \mathcal{K}_R}{\partial \omega} \right)^{-1} \mathcal{U}. \tag{5.16}$$

For a rotating Alfvén wave, this energy density  $\mathcal{U}$  has three distinct components:

$$\mathcal{U} = \frac{\langle B^2 \rangle}{2\mu_0} + \frac{\varepsilon_0}{2} \langle (\mathbf{v} \times \mathbf{B}_0)^2 \rangle + \frac{\rho}{2} \langle v^2 \rangle, \tag{5.17}$$

where  $\langle \rangle$  indicates an average over the fast  $\omega$  oscillations. The first term on the right-hand side is the magnetic energy, the second term is the electric energy and the third term is the kinetic energy. This energy density can be rewritten using the Alfvén velocity  $V$  and the velocity of light  $c$  as

$$\mathcal{U} = \frac{\rho}{2} \left[ \langle v^2 \rangle \left( 1 + \frac{V^2}{c^2} \left( 1 + \frac{k_{\parallel}^2 c^2}{\omega^2} \right) \right) - \left\langle \left( \mathbf{v} \cdot \frac{\mathbf{V}}{c} \right)^2 \right\rangle \right]. \tag{5.18}$$

Combining equations (5.16), (5.17) and the relation between energy and angular momentum absorption, one finally gets

$$\Gamma = 2\rho \frac{m}{\omega} \mathcal{K}_I \left( \frac{\partial \mathcal{K}_R}{\partial \omega} \right)^{-1} \left[ \langle v^2 \rangle \left( 1 + \frac{V^2}{c^2} \left( 1 + \frac{k_{\parallel}^2 c^2}{\omega^2} \right) \right) - \frac{\langle (\mathbf{v} \cdot \mathbf{V})^2 \rangle}{c^2} \right], \tag{5.19}$$

where  $\mathcal{K}_R$  and  $\mathcal{K}_I$  are given by (5.10) and  $\mathbf{v}$  is given by (3.26).

### 6. Conclusion

Building on previous contributions studying Alfvén waves in rotating plasmas in geophysical and astrophysical settings, we have examined here the dynamics of OAM-carrying torsional Alfvén waves in a rotating plasma. It is found that two new couplings exist between the OAM of the Alfvén waves and the angular momentum of the rotating plasma.

One is Fresnel–Faraday rotation, that is, a rotation of the transverse structure of the wave due to the medium’s rotation, which had already been predicted for the high-frequency electronic modes that are Trivelpiece–Gould and Whistler–Helicon modes (Rax & Gueroult 2021). Extending these earlier contributions, direct Fresnel–Faraday rotation for torsional Alfvén waves in a rotating plasma is described by (4.11) and (4.13). It is the OAM analogue of the polarization drag effect for spin angular momentum waves

(Jones 1976; Player 1976). An important distinction found here, though, is that while rotation did not introduce new high-frequency modes so that Faraday–Fresnel rotation for Trivelpiece–Gould and Whistler–Helicon modes was simply the consequence of the interplay between Coriolis force and rotational Doppler shift (Rax & Gueroult 2021), the strong coupling to the inertial wave that exists for Alfvén waves in rotating plasmas makes this picture more complex.

The second coupling is the inverse effect through which the OAM-carrying wave exerts a torque on the plasma. Inverse Faraday–Fresnel rotation is described by (5.10) and (5.19). This inverse effect is akin to the spin angular momentum inverse Faraday effect but for the OAM of the wave. It is found that for a plasma with non-zero collisional absorption the damping of an OAM-carrying wave is the source of a torque on the plasma.

Looking ahead, these results suggest that direct Faraday–Fresnel rotation could in principle be used to diagnose plasma rotation with Alfvén waves. Conversely, it may be possible to utilize inverse Faraday–Fresnel rotation to sustain plasma rotation through Alfvén wave angular momentum absorption. The detailed analysis of these promising prospects, as well as the examination of the effect of radial non-uniformities, is left for future studies.

### Acknowledgements

The authors would like to thank Dr E.J. Kolmes, I.E. Ochs, M.E. Mlodik and T. Rubin for constructive discussions.

*Editor Tünde Fülöp thanks the referees for their advice in evaluating this article.*

### Funding

This work was supported by the US Department of Energy (N.J.F., grant no. ARPA-E, grant no. DE-AR001554); and the French National Research Agency (R.G., grant no. ANR-21-CE30-0002). J.-M.R. acknowledges Princeton University and the Andlinger Center for Energy + the Environment for the ACEE fellowship which made this work possible.

### Declaration of interest

The authors report no conflict of interest.

### REFERENCES

- ACHESON, D.J. 1972 On the hydromagnetic stability of a rotating fluid annulus. *J. Fluid Mech.* **52** (3), 529–541.
- ACHESON, D.J. & HIDE, R. 1973 Hydromagnetics of rotating fluids. *Rep. Progr. Phys.* **36** (2), 159–221.
- ALLEN, L., BARNETT, S.M. & PADGETT, M.J. 2016 *Optical Angular Momentum*. CRC Press.
- ALLEN, L., BEIJERSBERGEN, M.W., SPREEUW, R.J.C. & WOERDMAN, J.P. 1992 Orbital angular momentum of light and the transformation of laguerre-gaussian laser modes. *Phys. Rev. A* **45** (11), 8185–8189.
- ANDREWS, D.L. & BABIKER, M. (Eds.) 2012 *The Angular Momentum of Light*. Cambridge University Press.
- BEKHTENEV, A.A., VOLOSOV, V.I., PAL'CHIKOV, V.E., PEKKER, M.S. & YUDIN, Y.N. 1980 Problems of a thermonuclear reactor with a rotating plasma. *Nucl. Fusion* **20** (5), 579–598.
- BLIOKH, K.Y. & BLIOKH, Y.P. 2022 Momentum, angular momentum, and spin of waves in an isotropic collisionless plasma. *Phys. Rev. E* **105** (6), 065208.
- BLIOKH, K.Y., RODRIGUEZ-FORTUÑO, F.J., NORI, F. & ZAYATS, A.V. 2015 Spin–orbit interactions of light. *Nat. Photonics* **9** (12), 796–808.

- BONNEVIER, B. 1966 Diffusion due to ion-ion collisions in a multicomponent plasma. *Ark. Fys.* **33**, 255.
- BRILLOUIN, L. 1945 A theorem of Larmor and its importance for electrons in magnetic fields. *Phys. Rev.* **67** (7-8), 260–266.
- CAMPOS, L.M.B.C. 2010 On magnetoacoustic-gravity-inertial (MAGI) waves - I. Generation, propagation, dissipation and radiation. *Mon. Not. R. Astron. Soc.* **410** (2), 717–734.
- CHANDRASEKHAR, S. & KENDALL, P.C. 1957 On force-free magnetic fields. *Astrophys. J.* **126**, 457.
- CHANDRASEKHAR, S. & PRENDERGAST, K.H. 1956 The equilibrium of magnetic stars. *Proc. Natl Acad. Sci.* **42** (1), 5–9.
- FERMI, E. 1923 Sul trascinamento del piano di polarizzazione da parte di un messo rotante. *Rend. Mat. Accad. Lincei* **32**, 115–118, reprinted in *Collected Papers*, vol. 1 (University of Chicago Press, Chicago, 1962).
- FETTERMAN, A.J. & FISCH, N.J. 2008 Alpha channeling in a rotating plasma. *Phys. Rev. Lett.* **101** (20), 205003.
- FETTERMAN, A.J. & FISCH, N.J. 2010 Alpha channeling in rotating plasma with stationary waves. *Phys. Plasmas* **17** (4), 042112.
- FETTERMAN, A.J. & FISCH, N.J. 2011 The magnetic centrifugal mass filter. *Phys. Plasmas* **18** (9), 094503–3.
- FRANKE-ARNOLD, S., GIBSON, G., BOYD, R.W. & PADGETT, M.J. 2011 Rotary photon drag enhanced by a slow-light medium. *Science* **333** (6038), 65.
- GOEDBLOED, H., KEPPENS, R. & POEDTS, S. 2019 *Magnetohydrodynamics of Laboratory and Astrophysical Plasmas*. Cambridge University Press.
- GÖTTE, J.B., BARNETT, S.M. & PADGETT, M. 2007 On the dragging of light by a rotating medium. *Proc. R. Soc. A* **463** (2085), 2185.
- GUEROULT, R., FRUCHTMAN, A. & FISCH, N.J. 2013 Tendency of a rotating electron plasma to approach the brillouin limit. *Phys. Plasmas* **20** (7), 073505–7.
- GUEROULT, R., RAX, J.-M. & FISCH, N.J. 2014 The double well mass filter. *Phys. Plasmas* **21** (2), 020701.
- GUEROULT, R., RAX, J.-M. & FISCH, N.J. 2020 Enhanced tuneable rotatory power in a rotating plasma. *Phys. Rev. E* **102** (5), 051202(R).
- GUEROULT, R., RAX, J.-M. & FISCH, N.J. 2023 Wave propagation in rotating magnetised plasmas. *Plasma Phys. Control. Fusion* **65** (3), 034006.
- GUEROULT, R., RAX, J.-M., ZWEBEN, S. & FISCH, N.J. 2017 Harnessing mass differential confinement effects in magnetized rotating plasmas to address new separation needs. *Plasma Phys. Control. Fusion* **60**, 014018.
- GUEROULT, R., SHI, Y., RAX, J.-M. & FISCH, N.J. 2019a Determining the rotation direction in pulsars. *Nat. Commun.* **10** (1), 3232.
- GUEROULT, R., ZWEBEN, S.J., FISCH, N.J. & RAX, J.-M. 2019b *ExB* configurations for high-throughput plasma mass separation: an outlook on possibilities and challenges. *Phys. Plasmas* **26** (4), 043511.
- HAMEIRI, E. 1983 The equilibrium and stability of rotating plasmas. *Phys. Fluids* **26** (1), 230–237.
- HASSAM, A.B. 1997 Steady-state centrifugally confined plasmas for fusion. *Comments Plasma Phys. Control. Fusion* **18**, 263.
- HIDE, R. 1969 On hydromagnetic waves in a stratified rotating incompressible fluid. *J. Fluid Mech.* **39** (2), 283–287.
- JANES, G.S. 1965 Experiments on magnetically produced and confined electron clouds. *Phys. Rev. Lett.* **15** (4), 135–138.
- JANES, G.S., LEVY, R.H., BETHE, H.A. & FELD, B.T. 1966 New type of accelerator for heavy ions. *Phys. Rev.* **145** (3), 925–952.
- JANES, G.S., LEVY, R.H. & PETSCHKE, H.E. 1965 Production of BeV potential wells. *Phys. Rev. Lett.* **15** (4), 138–140.
- JONES, R.V. 1976 Rotary aether drag. *Proc. R. Soc. A* **349** (1659), 423–439.
- KRISHNAN, M., GEVA, M. & HIRSHFIELD, J.L. 1981 Plasma centrifuge. *Phys. Rev. Lett.* **46** (1), 36–38.
- KULSRUD, R.M. 1999 A critical review of galactic dynamos. *Annu. Rev. Astron. Astrophys.* **37** (1), 37–64.
- LEHNERT, B. 1954 Magnetohydrodynamic waves under the action of the Coriolis force. *Astrophys. J.* **119**, 647.

- LIGHTHILL, J. 1980 *Waves in Fluids*. Cambridge University Press.
- MIESCH, M.S. & TOOMRE, J. 2009 Turbulence, magnetism, and shear in stellar interiors. *Annu. Rev. Fluid Mech.* **41** (1), 317–345.
- OCHS, I.E. & FISCH, N.J. 2017 Particle orbits in a force-balanced, wave-driven, rotating torus. *Phys. Plasmas* **24**, 092513.
- OHKAWA, T. & MILLER, R.L. 2002 Band gap ion mass filter. *Phys. Plasmas* **9** (12), 5116–5120.
- PADGETT, M., WHYTE, G., GIRKIN, J., WRIGHT, A., ALLEN, L., ÖHBERG, P. & BARNETT, S.M. 2006 Polarization and image rotation induced by a rotating dielectric rod: an optical angular momentum interpretation. *Opt. Lett.* **31** (14), 2205.
- PLAYER, M.A. 1976 On the dragging of the plane of polarization of light propagating in a rotating medium. *Proc. R. Soc. A* **349** (1659), 441.
- RAX, J.-M. & GUEROULT, R. 2021 Faraday–Fresnel rotation and splitting of orbital angular momentum carrying waves in a rotating plasma. *J. Plasma Phys.* **87** (5), 905870507.
- RAX, J.-M. & ROBICHE, J. 2010 Theory of unfolded cyclotron accelerator. *Phys. Plasmas* **17** (10).
- RAX, J.M., GUEROULT, R. & FISCH, N.J. 2017 Efficiency of wave-driven rigid body rotation toroidal confinement. *Phys. Plasmas* **24** (3), 032504.
- RAX, J.M., GUEROULT, R. & FISCH, N.J. 2023 Quasilinear theory of Brillouin resonances in rotating magnetized plasmas. *J. Plasma Phys.* **89** (4), 905890408.
- SHINOHARA, S. & HORII, S. 2007 Initial trial of plasma mass separation by crossed electric and magnetic fields. *Japan. J. Appl. Phys.* **46** (7R), 4276.
- SHUKLA, P. 2012 Twisted shear Alfvén waves with orbital angular momentum. *Phys. Lett. A* **376** (44), 2792–2794.
- STENZEL, R.L. 2019 Whistler modes excited by magnetic antennas: a review. *Phys. Plasmas* **26** (8), 080501.
- STENZEL, R.L. & URRUTIA, J.M. 2014 Magnetic antenna excitation of Whistler modes. II. Antenna arrays. *Phys. Plasmas* **21** (12), 122108.
- STENZEL, R.L. & URRUTIA, J.M. 2015a Helicon modes in uniform plasmas. III. Angular momentum. *Phys. Plasmas* **22** (9), 092113.
- STENZEL, R.L. & URRUTIA, J.M. 2015b Helicon waves in uniform plasmas. II. High m numbers. *Phys. Plasmas* **22** (9), 092112.
- STENZEL, R.L. & URRUTIA, J.M. 2015c Magnetic antenna excitation of whistler modes. IV. Receiving antennas and reciprocity. *Phys. Plasmas* **22** (7), 072110.
- STENZEL, R.L. & URRUTIA, J.M. 2018 Helicons in uniform fields. II. Poynting vector and angular momenta. *Phys. Plasmas* **25** (3), 032112.
- STIX, T.H. 1992 *Waves in Plasmas*. AIP Press.
- TAYLOR, J.B. 1989 Current drive by plasma waves and helicity conservation. *Phys. Rev. Lett.* **63** (13), 1384–1385.
- THAURY, C., GUILLAUME, E., CORDE, S., LEHE, R., LE BOUTELLER, M., TA PHUOC, K., DAVOINE, X., RAX, J.M., ROUSSE, A. & MALKA, V. 2013 Angular-momentum evolution in laser-plasma accelerators. *Phys. Rev. Lett.* **111** (13), 135002.
- THOMSON, J.J. 1885 Note on the rotation of the plane of polarization of light by a moving medium. *Proc. Camb. Phil. Soc.* **5**, 250.
- URRUTIA, J.M. & STENZEL, R.L. 2015 Magnetic antenna excitation of whistler modes. III. Group and phase velocities of wave packets. *Phys. Plasmas* **22** (7), 072109.
- URRUTIA, J.M. & STENZEL, R.L. 2016 Helicon waves in uniform plasmas. IV. Bessel beams, Gendrin beams, and helicons. *Phys. Plasmas* **23** (5), 052112.
- WILCOX, J.M. 1959 Review of high-temperature rotating-plasma experiments. *Rev. Mod. Phys.* **31** (4), 1045–1051.
- WISNIEWSKI-BARKER, E., GIBSON, G.M., FRANKE-ARNOLD, S., BOYD, R.W. & PADGETT, M.J. 2014 Mechanical Faraday effect for orbital angular momentum-carrying beams. *Opt. Express* **22** (10), 11690.
- YOSHIDA, Z. 1991 Discrete eigenstates of plasmas described by the Chandrasekhar-Kendall functions. *Prog. Theor. Phys.* **86** (1), 45–55.